



High optical quality Y_2O_3 transparent ceramics with fine grain size fabricated by low temperature air pre-sintering and post-HIP treatment

Zhongying Wang^a, Le Zhang^b, Hao Yang^b, Jian Zhang^{b,*}, Lixi Wang^a, Qitu Zhang^{a,*}

^aCollege of Materials Science and Engineering, Nanjing Tech University, Nanjing 210009, China

^bJiangsu Key Laboratory of Advanced Laser Materials and Devices, School of Physics and Electronic Engineering, Jiangsu Normal University, Xuzhou 221116, China

Received 28 October 2015; received in revised form 18 November 2015; accepted 18 November 2015

Available online 27 November 2015

Abstract

High optical quality Y_2O_3 transparent ceramics with fine grain size were successfully fabricated by air pre-sintering at various temperature ranging from 1500 to 1600 °C combined with a post-hot-isostatic pressing (HIP) treatment using co-precipitated powders as the starting material. The fully dense Y_2O_3 transparent ceramic with highest transparency was obtained by pre-sintered at 1550 °C for 4 h in air and post-HIPed at 1600 °C for 3 h (the pressure of HIP 200 MPa), and it had fine microstructure and the average grain size was 0.96 μm . In addition, the in-line transmittance of the ceramic reached 81.7% at 1064 nm (1 mm thickness). By this approach, the transparent Y_2O_3 ceramics with fine grain size (< 1.6 μm) were elaborated without any sintering aid.

© 2015 Elsevier Ltd and Techna Group S.r.l. All rights reserved.

Keywords: High optical quality; Air pre-sintering; Post-HIP treatment; Fine microstructure

1. Introduction

Y_2O_3 transparent ceramic has been widely used as laser host materials, infrared domes, high temperature chemical-resistant substrates and component of semiconductor equipment, due to its excellent properties such as high melting point (2430 °C), broad range of optical transparency (0.2–8 μm), high physical and chemical stabilities, and strong resistance properties for fluorine-based plasmas [1,2].

To obtain high optical quality Y_2O_3 ceramics, H_2 gas sintering or vacuum sintering techniques at 1750 °C or even high temperature were generally necessary for completing the densification process [3]. In addition, various sintering aids such as HfO_2 , ThO_2 and ZrO_2 were also used to suppress the abnormal grain growth at the final densification process. Furthermore, in these approaches, the heating elements such as tungsten mesh or rod in the sintering furnace are very expensive. Recently, Ballato

et al. [4,5], reported the Y_2O_3 transparent ceramics with good optical quality could be fabricated at a relatively lower sintering temperature by two-step sintering process and followed by the post-HIP treatment. Because of no adopted sintering aid, the segregation of second phase at the grain boundary area was maximally avoided at high sintering temperature. However, in their experiment, the sintering of transparent ceramics still needed the expensive vacuum furnace.

Huang et al. [6] also reported a novel sintering method for Y_2O_3 transparent ceramics. The ceramics were sintered in O_2 atmosphere and the sintering temperature was as low as 1600–1650 °C. In addition, the influence of ZrO_2 as the sintering aid on the densification of Y_2O_3 ceramics was also investigated, and 0.5–2.0 at% ZrO_2 was added to obtain the high transparency.

Furthermore, the pre-sintering could promote the green body to achieve a certain degree of densification before the post-HIP treatment [7,8], but the air pre-sintering of Y_2O_3 ceramics is always ignored easily due to the low efficiency on densification compared with vacuum pre-sintering. Moreover, it is different with vacuum pre-sintering, and that does not need the expensive instrument and apparatus, which is an energy-saving

*Corresponding authors.

E-mail addresses: jzhang@jsnu.edu.cn (J. Zhang),
[njzqt@126.com](mailto:njqzt@126.com) (Q. Zhang).

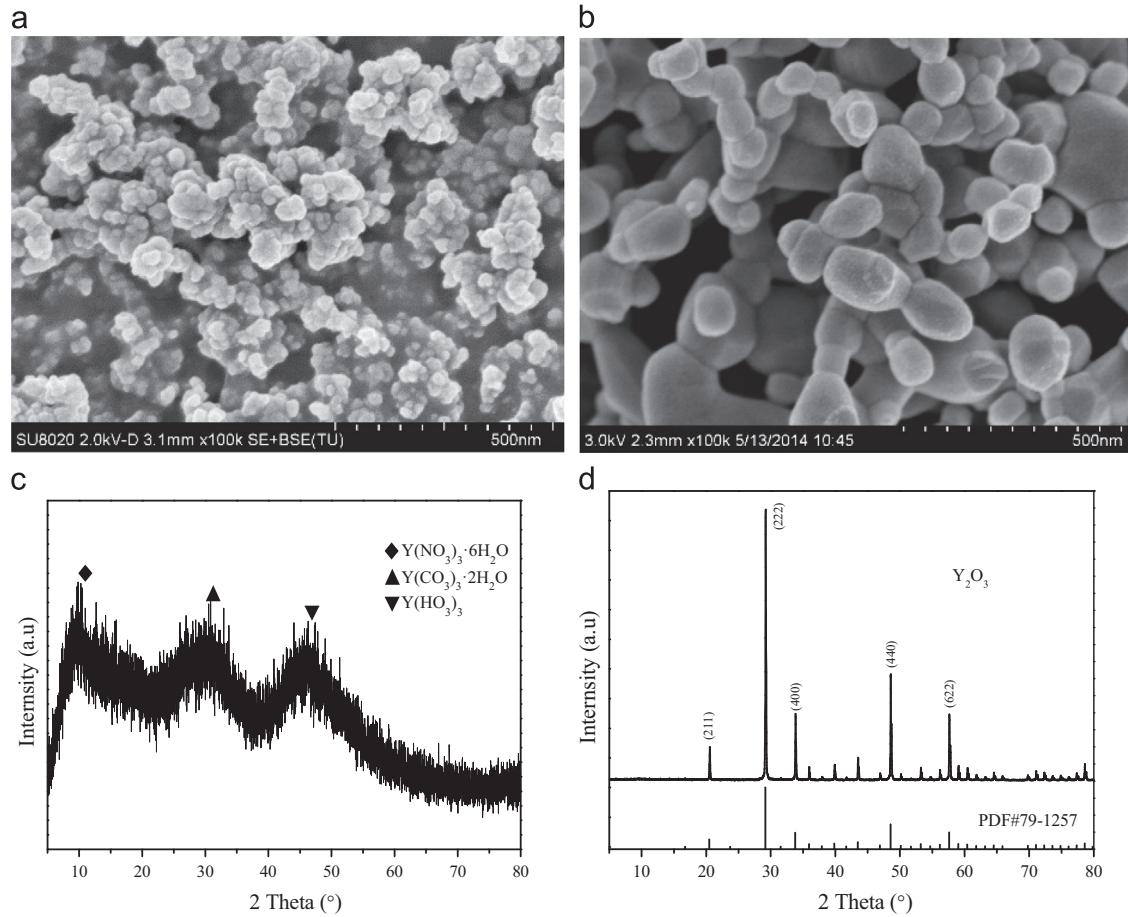


Fig. 1. FESEM images of (a) precursors and (b) Y_2O_3 powders calcined at $1300\text{ }^\circ\text{C}$ for 3 h and XRD patterns of (c) precursors and (d) Y_2O_3 powders calcined at $1300\text{ }^\circ\text{C}$ for 3 h.

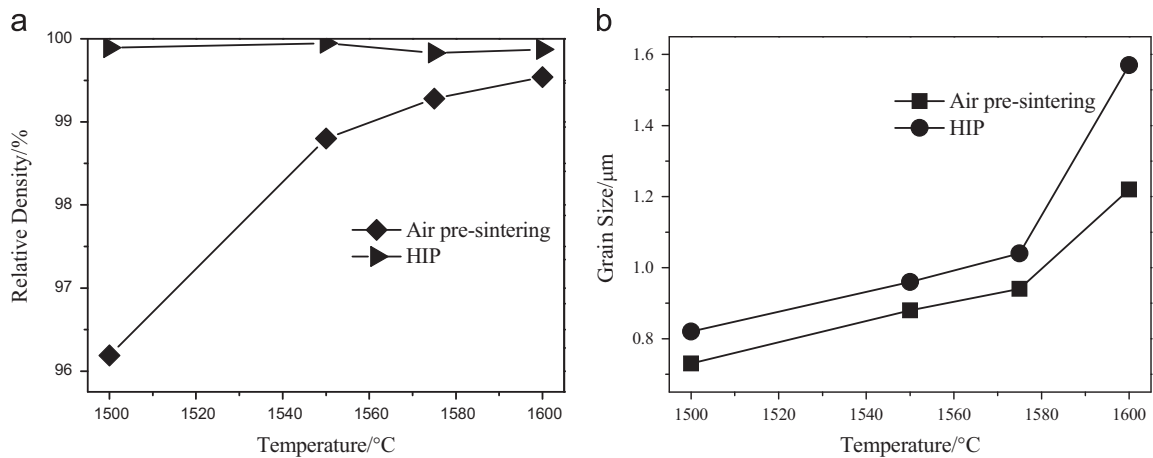


Fig. 2. (a) Relative densities and (b) grain sizes of Y_2O_3 under different air pre-sintering temperatures and $1600\text{ }^\circ\text{C}$ HIP.

and effective process without further annealing to compensate the oxygen vacancy that formed during the vacuum sintering process. Currently, numerous studies about the fabrication of transparent ceramic by vacuum pre-sintering and post-HIP treatment had been carried out [9], but fewer investigation of the preparation of Y_2O_3 transparent ceramic by air pre-

sintering combined with the post-HIP treatment has been systematically reported.

In present study, the nanocrystalline Y_2O_3 powders were synthesized by the co-precipitation method as the raw materials. By using the powders, the Y_2O_3 transparent ceramics were fabricated by the combination of air pre-sintering and the post-

HIP treatment. And the influence of the pre-sintering temperature on the microstructure and transparency of the ceramics without any sintering aid was systematically investigated.

2. Materials and experimental details

2.1. Synthesis of nanocrystalline Y_2O_3 powders

The $Y(NO_3)_3$ solution was prepared by dissolving yttria powders (99.999%, Alfa Aesar, Ward Hill, MA) with proper amount of nitric acid (analytical grades, Aladdin chemicals, Shanghai, China), then the solution was diluted with distilled water to a concentration of 0.15 M with 28 mol% ammonium sulfate (AS) (analytical grades, Aladdin chemicals, Shanghai, China). The mixed solution of 1.5 M ammonium hydrogen carbonate (AHC) and 2 M ammonia water (AW) (analytical grades, Aladdin chemicals, Shanghai, China) was used as the precipitant. The precursors were prepared by normal strike co-precipitation with 2 ml/min at 440 r/min, and then they were calcined at 1300 °C for 3 h to obtain the nanocrystalline Y_2O_3 powders.

2.2. Compaction and sintering of Y_2O_3 ceramic samples

The calcined Y_2O_3 powders were sieved through 200-mesh and then dry-pressed into $\Phi 15$ mm disk in a stainless steel mold at

25 MPa, followed by cold isostatic pressed at 200 MPa for 5 min. After removing the residue organics by calcined at 850 °C for 5 h, the compacted green bodies were pre-sintered at 1500 °C, 1550 °C, 1575 °C and 1600 °C respectively for 4 h in air. Finally, the pre-sintered samples were post-HIPed at 1600 °C for 3 h under 200 MPa in argon atmosphere. The Y_2O_3 transparent ceramics were obtained after coarse grinded and optical polished.

2.3. Characterizations

The morphology of the precursor and the calcined powders were performed by using a field emission scanning electron microscopy (FESEM, S4800, Hitachi, Japan). The Phases of the precursor and Y_2O_3 powders were identified by the X-ray diffraction (XRD, D2, Bruker, Germany). The relative densities of ceramics were measured by the Archimedes method with the theoretical density of Y_2O_3 as 5.031 g/cm³. Microstructural investigation of the sintered ceramic specimens was carried out by a scanning electron microscope (SEM, JSM-6510, JEOL, Japan). The measurement of the in-line transmittance of the as-prepared ceramics was obtained by using a UV–vis–NIR spectrophotometer (Lambda 950, Perkin-Elmer, Waltham, MA) in the wavelength range of 200–1500 nm.

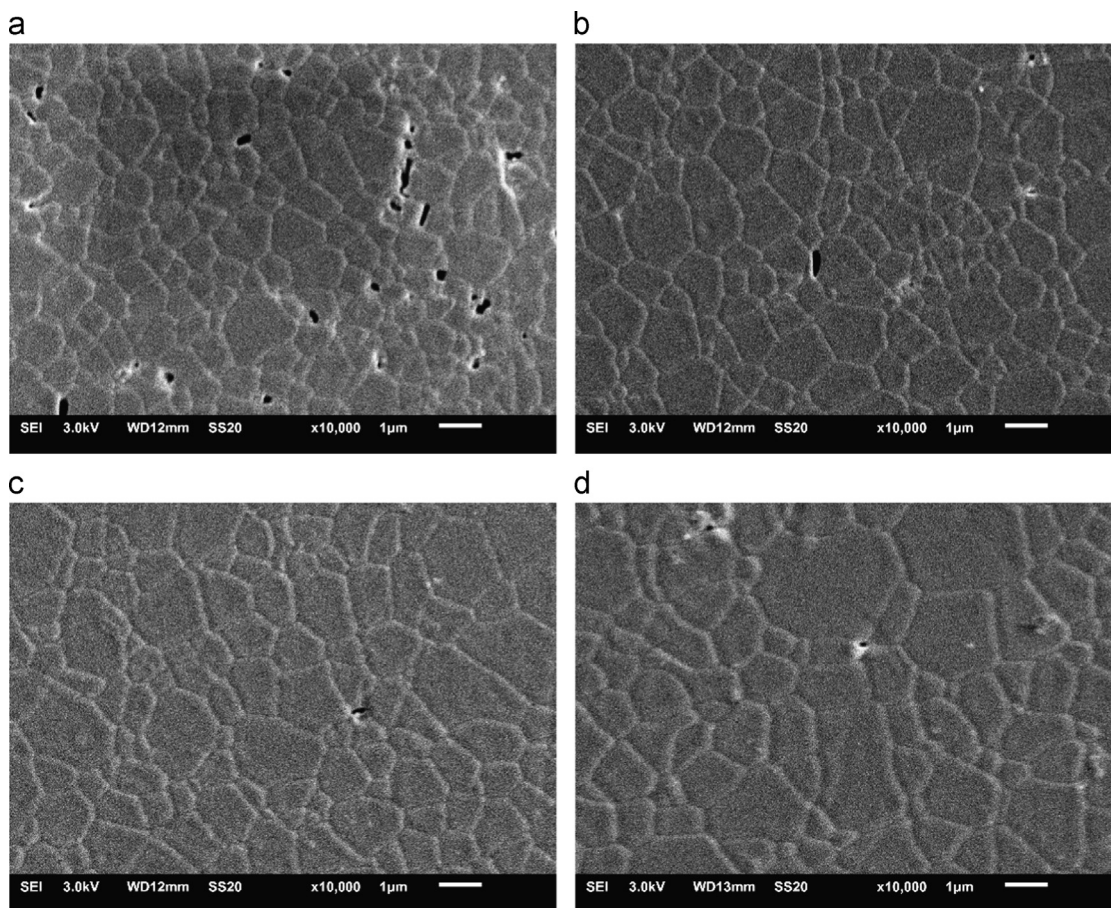


Fig. 3. SEM images of the thermal etched surfaces of air pre-sintered Y_2O_3 ceramics at (a) 1500 °C; (b) 1550 °C; (c) 1575 °C and (d) 1600 °C for 4 h.

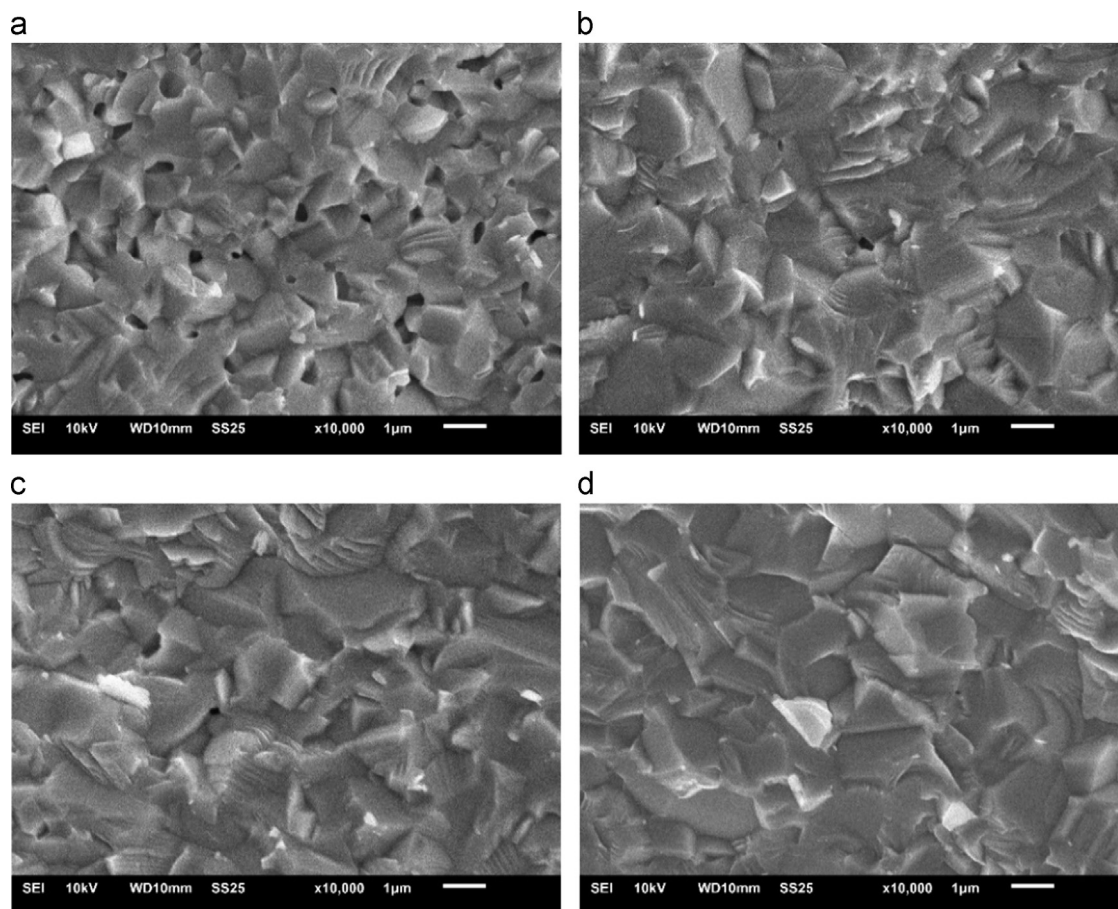


Fig. 4. SEM images of the fracture surfaces of air pre-sintered Y_2O_3 ceramics at (a) 1500 °C; (b) 1550 °C; (c) 1575 °C and (d) 1600 °C all for 4 h.

3. Results and discussion

3.1. Characterization of Y_2O_3 powders

To obtain fine grain size Y_2O_3 ceramics with high density, the dispersible nanocrystalline Y_2O_3 powders are necessary. It was reported that the nanocrystalline Y_2O_3 powders with good sintering activity could be synthesized by the coprecipitation method [10]. Fig. 1 shows the FESEM images and XRD patterns of the precursors and as-prepared Y_2O_3 powders. In Fig. 1(c), the XRD pattern of precursors indicates that a large amount of $Y(NO_3)_3 \cdot 6H_2O$, $Y(CO_3)_3 \cdot 2H_2O$ and a little $Y(OH)_3$ existed in the precursors. In Fig. 1(a), the granular precursors were $Y_2(CO_3)_3 \cdot 2H_2O$, but needle-like $Y(OH)_3$ could not be found nearly, and $Y_2(CO_3)_3 \cdot 2H_2O$ was beneficial for high sintering activity of calcined powders [11]. The mean particle size of calcined Y_2O_3 powders at 1300 °C was about 120 nm in Fig. 1(b), but existing slight agglomeration was negative for the sintering activity to a certain extent. Compared with the standard card (PDF79–1257, Ia3), the powders presented a single cubic Y_2O_3 phase and no any impurity phases could be observed at the calcined temperature of 1300 °C in Fig. 1(d). The as-prepared nanocrystalline Y_2O_3 powders provided the better basis to obtain high optical quality Y_2O_3 transparent ceramics with fine microstructure.

3.2. Effect of air pre-sintering and post-HIP treatment on relative densities and grain sizes

Fig. 2(a) shows the relative densities of Y_2O_3 ceramics after air pre-sintering and post-HIP treatment, respectively. When the pre-sintering was at 1500 °C, the relative density of the sample was only 96.2%. However, it significantly increased to 99% at the pre-sintering temperature of 1550 °C. Furthermore, it increased to 99.5% that was too dense when pre-sintering was at 1600 °C. And the samples were quite compact and slightly translucent. In addition, after the post-HIP treatment at 1600 °C in Fig. 2(a), all post-HIPed Y_2O_3 ceramics that pre-sintered at the different temperatures had the similar high relative densities. In particular, the relative density of the pre-sintering Y_2O_3 ceramic at 1550 °C with the post-HIP treatment was highest that reached to 99.9%. Moreover, the grain growth happened during the post-HIP treatment in Fig. 2(b), and the extra 200 MPa of argon atmosphere supplied driven force for the grain growth, which greatly enhanced the densification rate of the Y_2O_3 ceramics.

3.3. Effect of different pre-sintering temperatures on the microstructure of Y_2O_3 ceramics

Before the post-HIP treatment, the pre-sintering body should reach the closed porosity. In addition, in order to obtain the

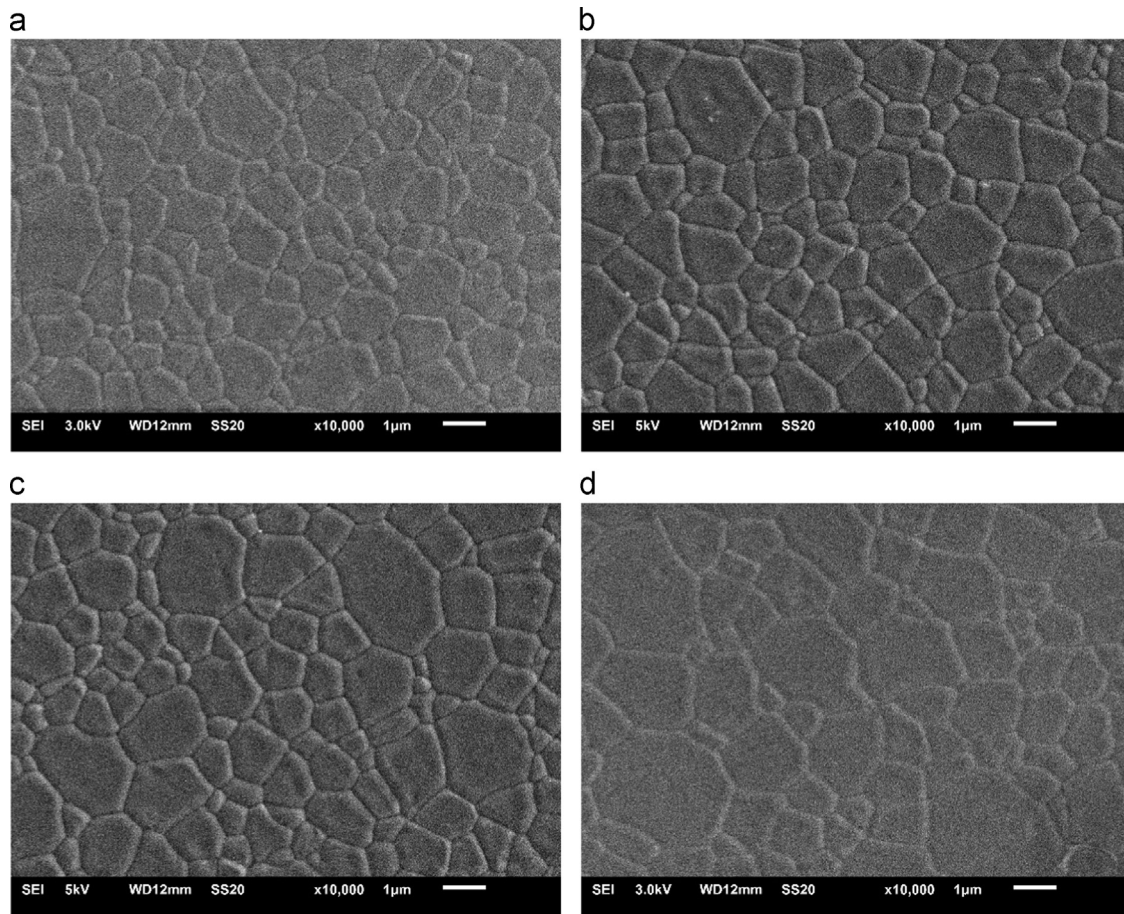


Fig. 5. SEM images of the thermal etched surfaces of post-HIP treated Y_2O_3 ceramics at 1600 °C for 3 h after pre-sintering at (a) 1500 °C; (b) 1550 °C; (c) 1575 °C and (d) 1600 °C all for 4 h.

high optical transparency, the pores trapped in the grains should be maximally released during the pre-sintering process. The SEM images of thermal-etched surfaces of the pre-sintered Y_2O_3 ceramics at different temperatures are shown in Fig. 3. A large number of intergranular pores that connected together were observed in the Y_2O_3 ceramic pre-sintered at 1500 °C with relative density of 96.2% in Fig. 3(a). When the pre-sintering temperature increased to 1550 °C, the number of intergranular pores decreased dramatically. The pores tended to be isolated and mainly existed nearby crystal grains in Fig. 3 (b). Fig. 3(c) presented the SEM picture of Y_2O_3 ceramic pre-sintered at 1575 °C, and the size of the pores decreased sharply with increasing the pre-sintering temperature. When the pre-sintering temperature was 1600 °C (Fig. 3(d)), the intergranular pores emerged among the grain boundaries.

In addition, the average grain size of the pre-sintered Y_2O_3 ceramic at 1600 °C was about 1.22 μm in Fig. 2(b). With the pre-sintering temperature increased from 1500 °C, 1550 °C to 1575 °C, the average grain sizes of Y_2O_3 ceramics were from 0.73 μm , 0.88 μm to 0.94 μm , respectively. The previous study demonstrated that the grain growth behavior of dense Y_2O_3 with grain size of 0.3 ~ 12.5 μm was described by the parabolic law [12]:

$$d^2 - d_0^2 = 2M\gamma(t - t_0) \quad (1)$$

where d_0/d is the grain size at time t_0/t , respectively. γ represents the grain boundary energy, and M means the grain boundary mobility. Therefore, at 1600 °C, the pre-sintered ceramic has higher grain boundary energy and mobility.

Fig. 4 shows the SEM images of the fracture surfaces of samples at different pre-sintering temperature. Obviously, the pores were all on the grain boundaries in Fig. 4(a), and the size of single pore was close to that of half grain. In addition, most pores were connected with each other, which was consistent with the results observed in the thermal etched surface shown in Fig. 3(a). When pre-sintering temperature increased to 1600 °C, nearly no pores could be found and the microstructure was almost dense. And the grains also quickly grown up with increasing the pre-sintering temperature on the fracture surfaces.

3.4. Effect of the post-HIP treatment on microstructure of Y_2O_3 ceramics

To observe the microstructural changes of the Y_2O_3 ceramics after the post-HIP treatment, the thermal etched surfaces and fracture surfaces of the as-prepared samples were characterized by SEM. Fig. 5 shows the thermal etched surfaces of Y_2O_3 ceramics that post-HIPed at 1600 °C after pre-sintered at various

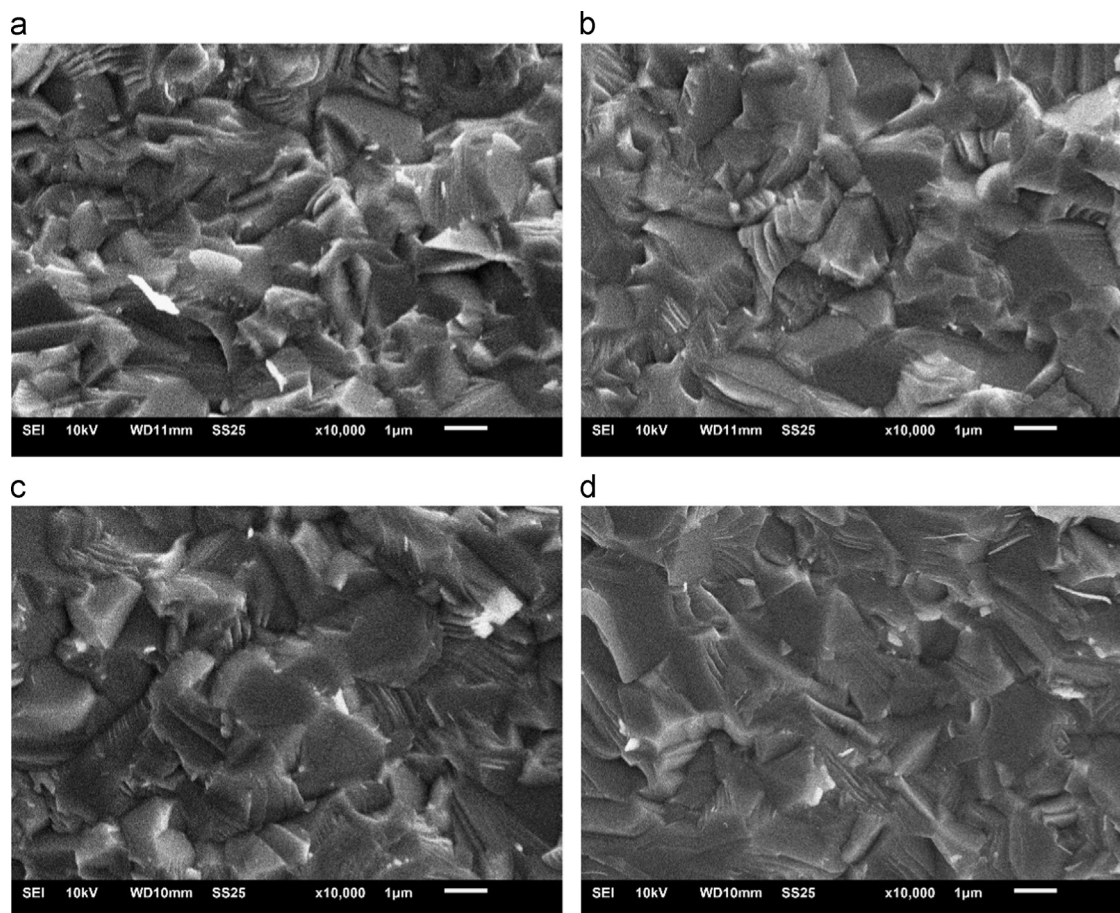


Fig. 6. SEM images of the fracture surfaces of post-HIP treated Y_2O_3 ceramics at 1600 °C for 3 h after pre-sintering at (a) 1500 °C; (b) 1550 °C; (c) 1575 °C and (d) 1600 °C all for 4 h.

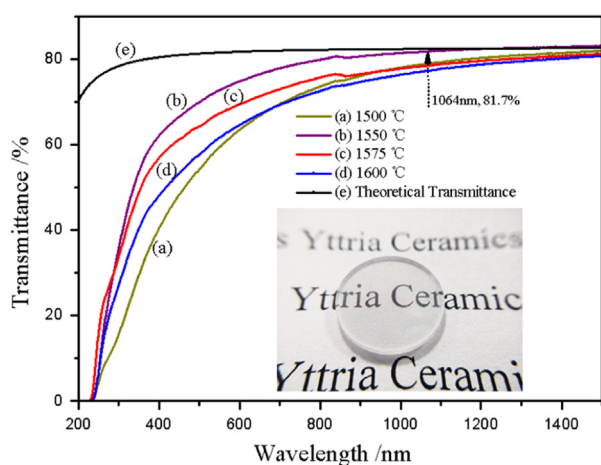


Fig. 7. In-line transmittance of HIPed Y_2O_3 ceramics at 1600 °C that pre-sintered at (a) 1500 °C, (b) 1550 °C, (c) 1575 °C and (d) 1600 °C and (e) theoretical transmittance (the picture of sample (b), 1 mm thickness).

temperatures. After the post-HIP treatment, the full dense Y_2O_3 ceramics were obtained and the average grain size of Y_2O_3 ceramic increased. And the average grain sizes of ceramics increased from 0.82 μm to 1.57 μm with the pre-sintering temperature increased from 1500 °C to 1600 °C. Meanwhile, all Y_2O_3 ceramics became transparent which was a very crucial

achievement. For the fabrication of transparent ceramics, it is very important to remove the residue pores completely. From the above results, it can be found that the post-HIP treatment is very effective for fabricating the transparent Y_2O_3 ceramics, when proper pre-sintering conditions are selected [13].

Fig. 6 shows the SEM pictures of the fracture surfaces of Y_2O_3 ceramics after the post-HIP treatment. Not any pore was observed, and the dense microstructures presented. This was consistent with the information shown in Fig. 5.

Although the topography and distribution of the porosity was highly thermodynamically unfavorable, the post-HIP treatment caused the intergranular porosity to disappear effectively [14]. Sintering was advanced by the application of the external pressure was known to increase densification in comparison with coarsening through enhanced diffusion and possibly by plastic deformation. An applied compressive stress decreases the concentration of vacancies at grain boundaries and hence increases mass transport by diffusion to the pores, because of the vacancy concentration gradient [15].

In the case of HIP, where external pressure results in pore shrinkage, the mobility for shrinkage is governed by the plastic deformation of surrounding grains. The ability of plastic deformation is significantly enhanced by a grain boundary sliding. It is known that the sliding activity increases with decreasing grain size [16]. Consequently, the pore shrinkage

by HIP is promoted in the fine-grained microstructure. And the fact that substantial grain growth took place during HIP can be certainly attributed to the high temperature and long dwell time, since there is no pinning effect exerted by pores to resist grain growth after removal of these latter [17].

Therefore, it was found that the average grain size of the sample pre-sintered and the post-HIPed all at 1600 °C was 1.57 μm that was larger than other three samples shown in Figs. 2(b) and 5. When the pre-sintering temperature was below 1600 °C, the samples were not impact with a large number of intergranular pores that need more energy to be consumed during the post-HIP treatment. In addition, in the post-HIP treatment, a certain faulty degree of densification that was achieved by pre-sintering prevented grains growing up in a sense. Researches had shown that pre-sintering also plays a very important role in the fabrication process while also having significant effects on the transparency and microstructure of transparent ceramics [18,19].

3.5. Effect of different air pre-sintering and post-HIP treatment on optical properties

The Fig. 7 shows the in-line transmittance of Y₂O₃ transparent ceramics. And the in-line transmittance of the sample that pre-sintered at 1550 °C and post-HIPed at 1600 °C was the highest, which reached 81.7% at 1064 nm (in Fig. 7(b), 1 mm thickness). Its photograph was posted in Fig. 7. And the theoretical transmittance of the Y₂O₃ transparent ceramic was presented in Fig. 7(e). For all samples pre-sintered at various temperatures, there was quite a drop of transparency at 250–800 nm compared with the curve of theoretical transmittance because of the small amount of residue tiny pores, which had obvious and important effects on the transparency near ultraviolet.

Normally, after high temperature sintering in vacuum, or hydrogen atmosphere, the black color of Y₂O₃ ceramics would be obtained, which have been extensively reported. The oxygen vacancies and color centers, formed during the high temperature sintering process, were considered to be the main reasons of black color. In order to obtain the transparent Y₂O₃ ceramics, long time annealing in air are necessary. Fortunately, in this work, the annealing in air to eliminate the vacancies and color centers could be ignored, and the samples were pre-sintered below 1600 °C in air and the post-HIP treatment temperature as low as 1600 °C were applied. Both of the pre-sintering temperature and post-HIP treatment temperature were much lower than the temperature applied in the known literature. Although more detail studies need to be carried out in future, it is very clear that the approach adopted in this work has the great potential.

4. Conclusions

In this paper, nanocrystalline Y₂O₃ powders as the starting materials by co-precipitation were used to prepare Y₂O₃ transparent ceramics by air pre-sintering and the post-HIP treatment. A relatively low air pre-sintering temperature effectively prevented the formation of intragranular pores that

resulted from the rapid grain growth. Therefore, appropriate pre-sintering in air was important to achieve ultimate higher optical quality of the samples followed by the post-HIP treatment. In the air pre-sintering process, the grains grown up to fine and appropriate size with the increase of temperature. However, after the same post-HIP treatment temperature of 1600 °C, only the grain size of the sample pre-sintered at 1600 °C increased to 1.57 μm distinctly.

The combination of air pre-sintering at 1550 °C for 4 h and post-HIP treatment at 1600 °C for 3 h resulted in the best high optical quality transparent Y₂O₃ ceramics in present study. The average grain size of the as-prepared Y₂O₃ ceramic was 0.96 μm, and the best in-line transmittance reached 81.7% at 1064 nm (1 mm thickness).

Acknowledgments

The authors acknowledge the generous financial support from Priority Academic Program Development of Jiangsu Higher Education Institutions (PAPD), and National Natural Science Foundation of China (51402133, 51202111).

References

- [1] M.S. He, J.B. Li, H. Lin, G.R. Guo, L. Liang, Fabrication of transparent polycrystalline yttria ceramics by combination of SPS and HIP, *J. Rare Earth* 24 (2006) 222–224.
- [2] J. Mouzon, A. Maitre, L. Frisk, N. Lehto, M. Oden, Fabrication of transparent yttria by HIP and the glass-encapsulation method, *J. Eur. Ceram. Soc.* 29 (2) (2009) 311–316.
- [3] J. Zhang, L.Q. An, M. Liu, S. Shimai, S.W. Wang, Sintering of Yb³⁺: Y₂O₃ transparent ceramics in hydrogen atmosphere, *J. Eur. Ceram. Soc.* 29 (2) (2008) 305–309.
- [4] K.S. Ballato, B. Yazgan Kokuoz, B. Kokuoz, Nanograined highly transparent yttria ceramics, *Opt. Lett.* 34 (7) (2009) 1032–1035.
- [5] J. Ballato, K. Serivalsatit, B. Kokuoz, B. Yazgan-Kokuoz, Synthesis, processing, and properties of submicrometer-grained highly transparent yttria ceramics, *J. Am. Ceram. Soc.* 93 (5) (2010) 1320–1325.
- [6] Y.H. Huang, D.L. Jiang, J.X. Zhang, Q.L. Lin, Z.G. Huang, Sintering of transparent yttria ceramics in oxygen atmosphere, *J. Am. Ceram. Soc.* 93 (10) (2010) 2964–2967.
- [7] S.H. Lee, E.R. Kupp, A.J. Stevenson, J.M. Anderson, G.L. Messing, X. Li, E.C. Dickey, J.Q. Dumm, V.K. Simonaitis-Castillo, G.J. Quarles, Hot isostatic pressing of transparent Nd:YAG ceramics, *J. Am. Ceram. Soc.* 92 (7) (2009) 1456–1463.
- [8] L. Gan, Y.J. Park, H. Kim, J.M. Kim, J.W. Ko, J.W. Lee, Effects of pre-sintering and annealing on the optical transmittance of Zr-doped Y₂O₃ transparent ceramics fabricated by vacuum sintering conjugated with post-hot-isostatic pressing, *Ceram. Int.* 41 (8) (2015) 9622–9627.
- [9] A. Ikesue, K. Kamata, K. Yoshida, Synthesis of transparent Nd-doped HfO₂-Y₂O₃ ceramics using HIP, *J. Am. Ceram. Soc.* 79 (2) (1996) 359–364.
- [10] B. Lu, J.G. Li, T.S. Suzuki, M. Estili, W.G. Liu, X.D. Sun, Y. Sakka, Controlled synthesis of layered rare-earth hydroxide nanosheets leading to highly transparent (Y_{0.95}Eu_{0.05})₂O₃ ceramics, *J. Am. Ceram. Soc.* 98 (5) (2015) 1413–1422.
- [11] Z. Huang, W. Guo, Y. Liu, Q.F. Huang, F. Tang, Y.G. Cao, Synthesis of Nd:Y₂O₃ nanopowders leading to transparent ceramics, *Mater. Chem. Phys.* 128 (1–2) (2011) 44–49.
- [12] P.L. Chen, I.W. Chen, Grain boundary mobility in Y₂O₃: defect mechanism and dopant effects, *J. Am. Ceram. Soc.* 79 (7) (1996) 1801–1809.

- [13] W. Zhang, T.C. Lu, B.Y. Ma, N. Wei, Z.W. Lu, F. Li, Y.B. Guan, X. T. Chen, W. Liu, L. Qi, Improvement of optical properties of Nd:YAG transparent ceramics by post-annealing and post hot isostatic pressing, *Opt. Mater.* 35 (12) (2013) 2405–2410.
- [14] M. Descamps, L. Boilet, G. Moreau, A. Tricoteaux, J.X. Lu, A. Leriche, V. Lardot, F. Cambier, Processing and properties of biphasic calcium phosphates bioceramics obtained by pressureless sintering and hot isostatic pressing, *J. Eur. Ceram. Soc.* 33 (7) (2013) 1263–1270.
- [15] S.N. Bagayev, A.A. Kaminskii, Y.L. Kopylov, V.B. Kravchenko, Problems of YAG nanopowders compaction for laser ceramics, *Opt. Mater.* 33 (5) (2011) 702–705.
- [16] M. Suarez, A. Fernandez, J.L. Menendez, M. Nygren, R. Torrecillas, Z. Zhao, Hot isostatic pressing of optically active Nd:YAG powders doped by a colloidal processing route, *J. Eur. Ceram. Soc.* 30 (6) (2010) 1489–1494.
- [17] K. Tsukuma, Transparent MgAl_2O_4 spinel ceramics produced by HIP post-sintering, *J. Ceram. Soc. Jpn.* 114 (1334) (2006) 802–806.
- [18] G. Toci, M. Vannini, M. Ciofini, A. Lapucci, A. Pirri, A. Ito, T. Goto, A. Yoshikawa, A. Ikesue, G. Alombert-Goget, Y. Guyot, G. Boulon, Nd^{3+} -doped Lu_2O_3 transparent sesquioxide ceramics elaborated by the Spark Plasma Sintering (SPS) method. Part 2: first laser output results and comparison with Nd^{3+} -doped Lu_2O_3 and Nd^{3+} - Y_2O_3 ceramics elaborated by a conventional method, *Opt. Mater.* 41 (2015) 12–16.
- [19] D. Galusek, J. Sedlacek, J. Chovanec, M. Michalkova, The influence of MgO , Y_2O_3 and ZrO_2 additions on densification and grain growth of submicrometre alumina sintered by SPS and HIP, *Ceram. Int.* 41 (8) (2015) 9692–9700.